H I-deficient galaxies in intermediate density environments

H. Dénes[1,2⋆], V. A. Kilborn[1], B. S. Koribalski[2], O. I. Wong[3]
[1] *Centre for Astrophysics & Supercomputing, Swinburne University of Technology, PO Box 218, Hawthorn, VIC 3122, Australia*
[2] *Australia Telescope National Facility, CSIRO Astronomy and Space Science, P.O. Box 76, Epping, NSW 1710, Australia*
[3] *International Centre for Radio Astronomy Research, The University of Western Australia M468, 35 Stirling Highway, Crawley, WA 6009, Australia*

Released 2002 Xxxxx XX

ABSTRACT

Observations show that spiral galaxies in galaxy clusters tend to have on average less neutral hydrogen (H I) than galaxies of the same type and size in the field. There is accumulating evidence that such H I-deficient galaxies are also relatively frequent in galaxy groups. An important question is, which mechanisms are responsible for the gas deficiency in galaxy groups. To gain a better understanding of how environment affects the gas content of galaxies, we identified a sample of six H I-deficient galaxies from the H I Parkes All Sky Survey (HIPASS) using H I-optical scaling relations. One of the galaxies is located in the outskirts of the Fornax cluster, four are in loose galaxy groups and one is in a galaxy triplet. We present new high resolution H I observations with the Australia Telescope Compact Array (ATCA) of these galaxies. We discuss the possible cause of H I-deficiency in these galaxies based on H I observations and various multi-wavelength data. We find that the galaxies have truncated H I disks, lopsided gas distribution and some show asymmetries in their stellar disks. We conclude that both ram pressure stripping and tidal interactions are important gas removal mechanisms in low density environments.

Key words: galaxies: evolution – galaxies: general – radio lines: galaxies – surveys.

- Five per cent (94) of the galaxies in the HIPASS parent sample are Hi-deficient with DEF > 0.6. We select the 6 most Hi-deficient late-type galaxies for high resolution Hi observations. These galaxies have Hi masses between 2 to 25.3*10^8Mc and roughly 3 to 12 times less Hi than expected from the R-band scaling relation.
- Наблюдения: Australia Telescope Compact Array (ATCA). Velocity resolution: 0.1 km/s.

HI- По каталогу HIPASS Optical counterparts catalogue (HOPCAT, Doyle et al. 2005)

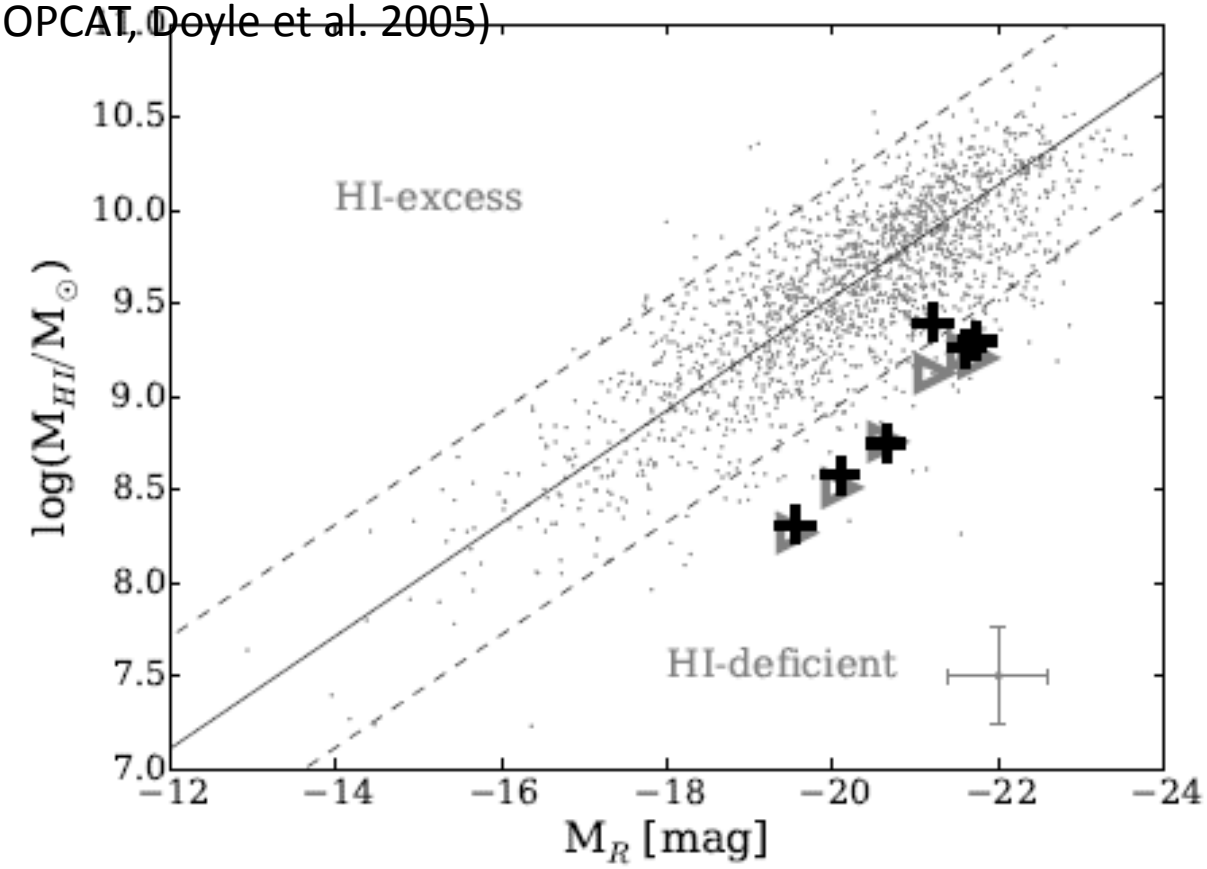

Figure 1. *R*-band magnitude versus H I mass for the parent sample. The solid line shows the *R*-band scaling relation from (Dénes et al. 2014) and the dashed line marks $DEF = \pm 0.6$. Grey triangles show the original HICAT H I data for the 6 sample galaxies and black crosses show the re-measured H I mass from the HIPASS data cubes (see Table 3). The error bar displayed in the bottom right indicates the average uncertainties in the data.

- One galaxy is in the outskirts of the Fornax cluster, four are in loose galaxy groups and one is ina triplet. We investigated the distance to the closest neighbouring galaxies in NED. None of the sample galaxies have signicant neighbours within 200 kpc projected distances.

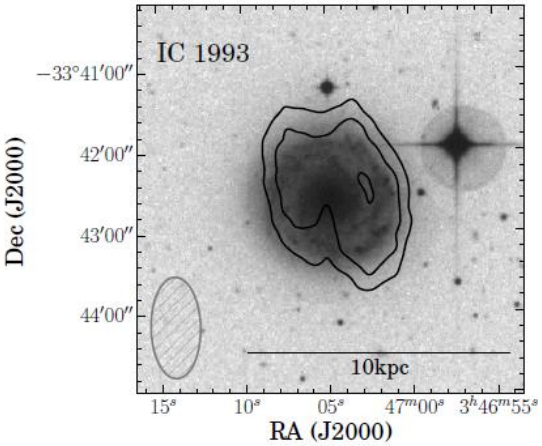
IC 1993
−33°41′00″
42′00″
43′00″
44′00″
Dec (J2000)
10kpc
15s 10s 05s 47m00s 3h46m55s
RA (J2000)

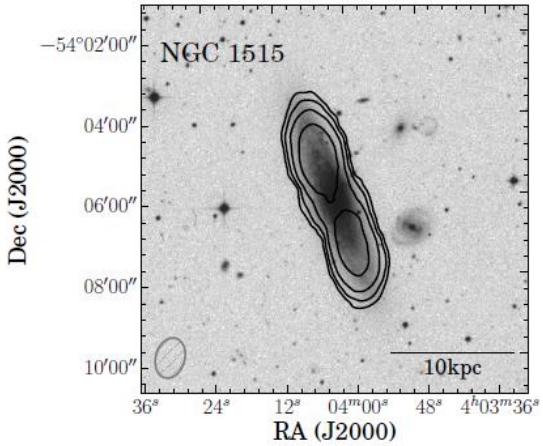
NGC 1515
−54°02′00″
04′00″
06′00″
08′00″
10′00″
Dec (J2000)
10kpc
36s 24s 12s 04m00s 48s 4h03m36s
RA (J2000)

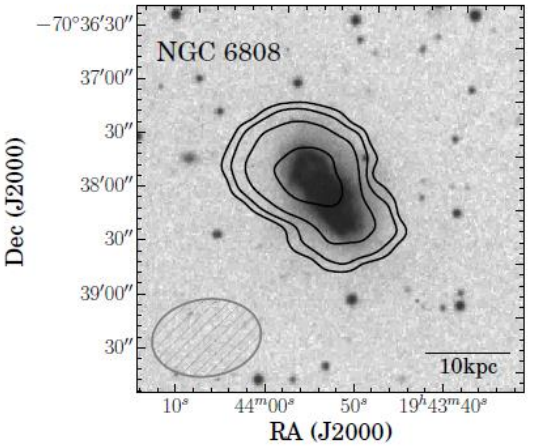
NGC 6808
−70°36′30″
37′00″
30″
38′00″
30″
39′00″
30″
Dec (J2000)
10kpc
10s 44m00s 50s 19h43m40s
RA (J2000)

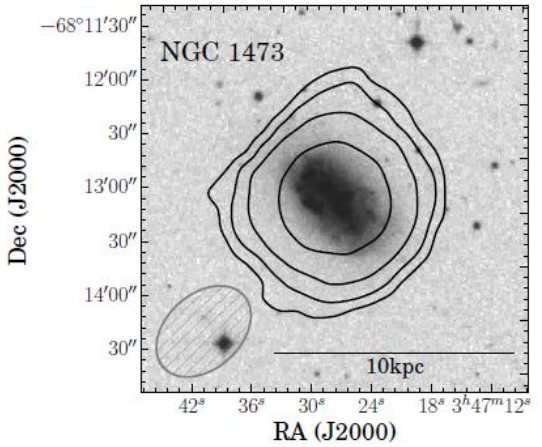
NGC 1473
−68°11′30″
12′00″
30″
13′00″
30″
14′00″
30″
Dec (J2000)
10kpc
42s 36s 30s 24s 18s 3h47m12s
RA (J2000)

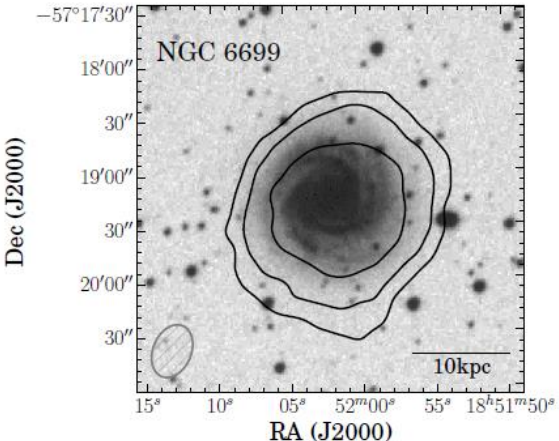
NGC 6699
−57°17′30″
18′00″
30″
19′00″
30″
20′00″
30″
Dec (J2000)
10kpc
15s 10s 05s 52m00s 55s 18h51m50s
RA (J2000)

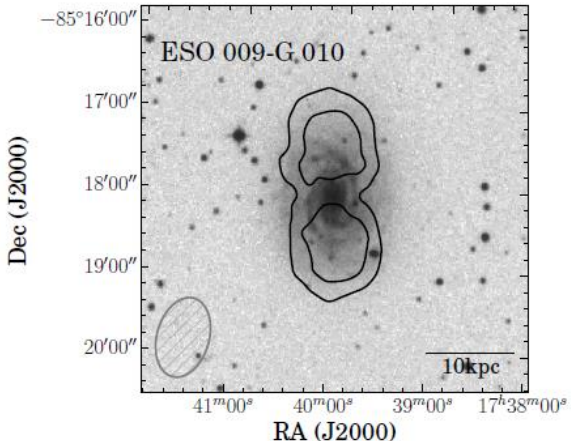
ESO 009-G 010
−85°16′00″
17′00″
18′00″
19′00″
20′00″
Dec (J2000)
10kpc
41m00s 40m00s 39m00s 17h38m00s
RA (J2000)

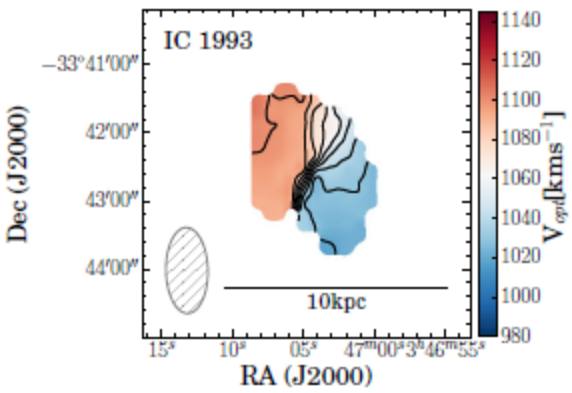
IC 1993
10kpc
Dec (J2000)
RA (J2000)
V_{opt}[kms^{-1}]

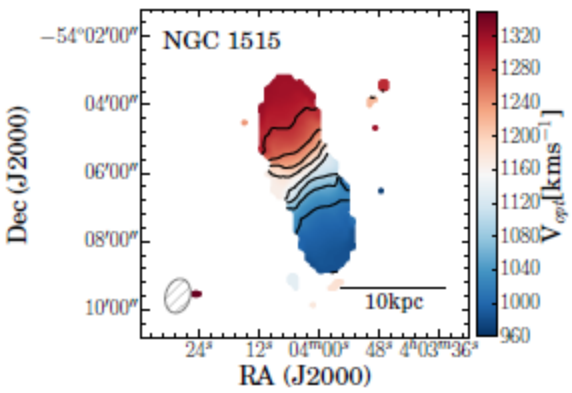
NGC 1515
10kpc
Dec (J2000)
RA (J2000)
V_{opt}[kms^{-1}]

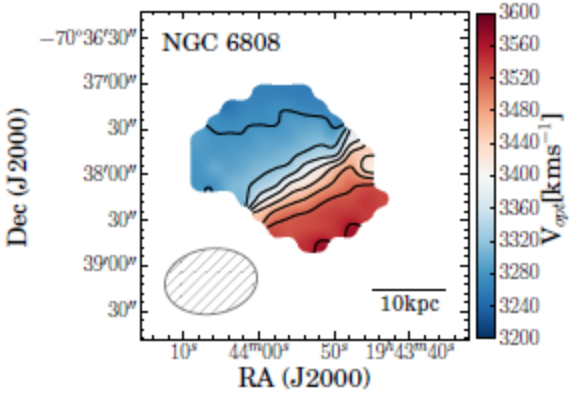
NGC 6808
10kpc
Dec (J2000)
RA (J2000)
V_{opt}[kms^{-1}]

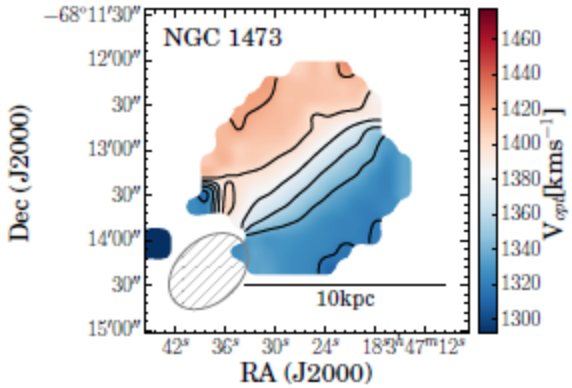
NGC 1473
10kpc
Dec (J2000)
RA (J2000)
V_{opt}[kms^{-1}]

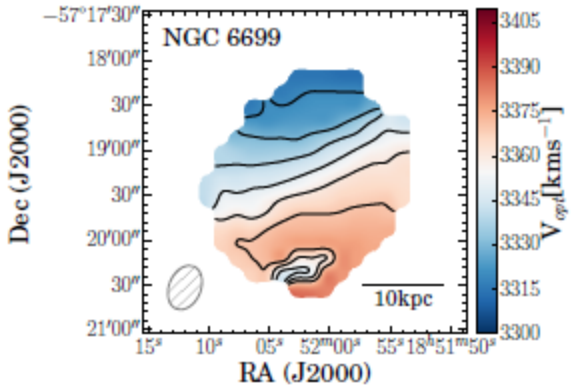
NGC 6699
10kpc
Dec (J2000)
RA (J2000)
V_{opt}[kms^{-1}]

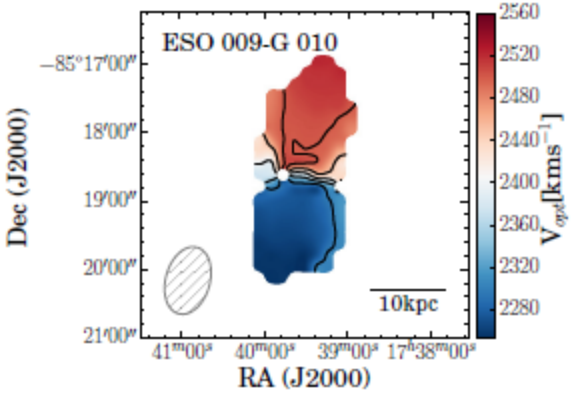
ESO 009-G 010
10kpc
Dec (J2000)
RA (J2000)
V_{opt}[kms^{-1}]

- Two galaxies, IC 1993 and NGC 6808 show strong asymmetries and almost all galaxies have a lopsided Hi distributions.
- NGC 6808 has a warped stellar disk which in combination with the strongly asymmetric Hi disk, clearly indicate strong tidal interactions in the recent past of this galaxy. Half the sample galaxies have slightly lopsided stellar disks, which can suggest tidal interactions

- We conclude that both ram pressure stripping and tidal interactions are important gas removal mechanisms in low density environments. Based on the star formation rates and the gas cycling times of the sample, strangulation is unlikely to be the main reason for Hi-deficiency.

Rotation Curve Decomposition for Size-Mass Relations of Bulge, Disk, and Dark Halo in Spiral Galaxies

Yoshiaki SOFUE
Institute of Astronomy, University of Tokyo, Mitaka, 181-0015 Tokyo, Japan
Email:*sofue@ioa.s.u-tokyo.ac.jp*

(Received ; accepted 2015)

Abstract

Rotation curves of more than one hundred spiral galaxies were compiled from the literature, and deconvolved into bulge, disk, and dark halo using χ^2 fitting in order to determine their scale radii and masses. Correlation analyses were obtained of the fitting parameters for galaxies that satisfied selection and accuracy criteria. Size-mass relations indicate that the sizes and masses are positively correlated among different components in such a way that the larger or more massive is the dark halo, the larger or more massive are the disk and bulge. Empirical size-mass relations were obtained for bulge, disk and dark halo by the least-squares fitting. The disk-to-halo mass ratio was found to be systematically greater by a factor of three than that predicted by cosmological simulations combined with photometry. A preliminary mass function for dark halo was obtained, which is represented by the Schechter function followed by a power law.

Key words: dark matter — galaxies: haloes — galaxies: kinematics and dynamics — galaxies: rotation curve — galaxies: spiral — galaxies: structure

1. Introduction

Decomposition of rotation curves into mass components of bulges, disks, and dark halos.

2. Compilation of Rotation Curves and

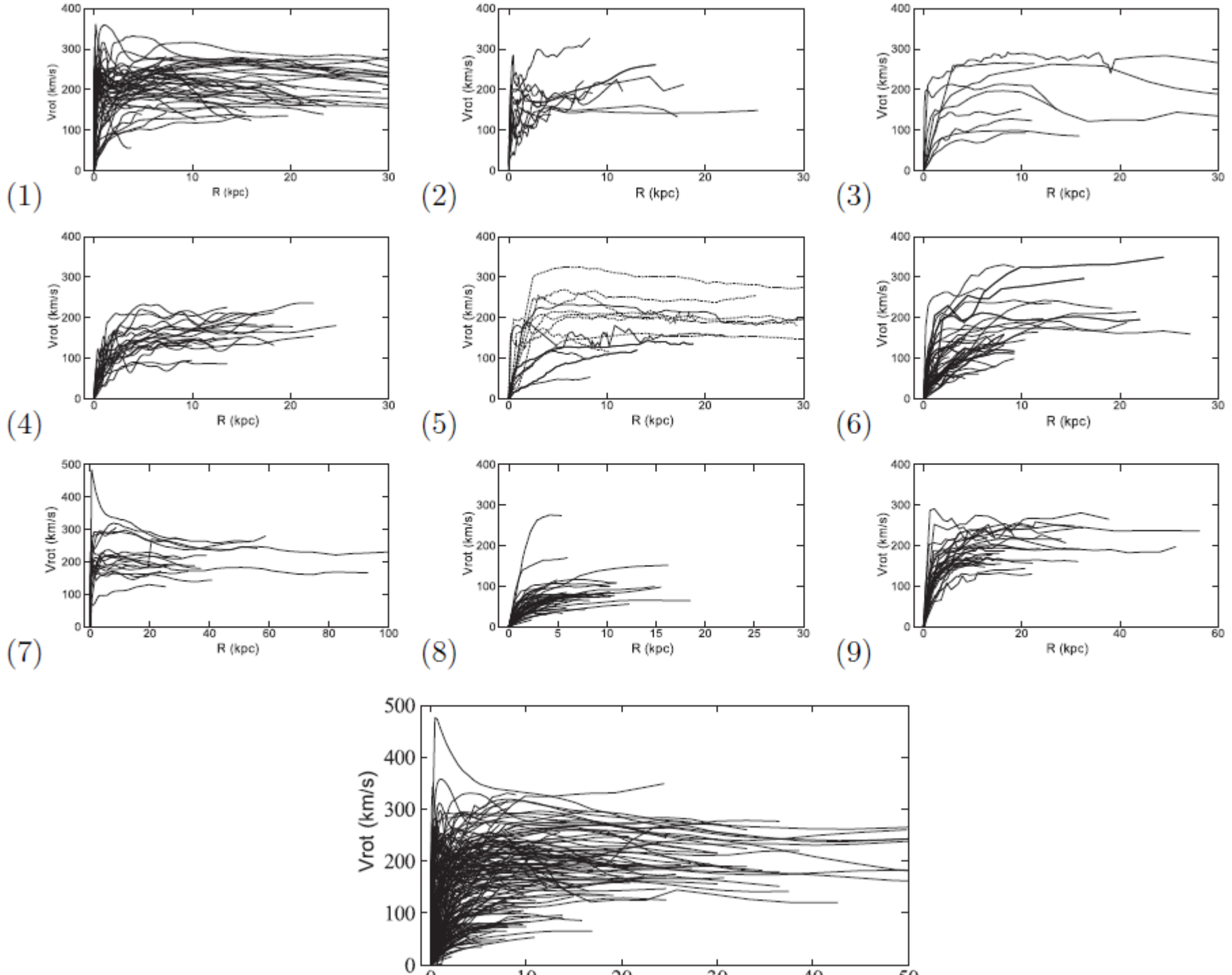
(1)
(2)
(3)
(4)
(5)
(6)
(7)
(8)
(9)
Vrot (km/s)
R (kpc)

Table 1. Dynamical parameters for selected spiral galaxies.

ame†	$r^{\ddagger}_{\rm max}$	$a_{\rm b}$(kpc)	$M_{\rm b}(10^{10}M_{\odot})$	$a_{\rm d}$(kpc)	$M_{\rm d}(10^{10}M_{\odot})$	h(kpc)	$M_{\rm h}(10^{10}M_{\odot})$	R_{200}(kpc)	$M_{200}(10^{10}M_{\odot})$
00000	469.6	1.52± 0.11	3.53± 0.33	5.9± 0.1	9.2± 0.4	14.7± 0.4	9.2± 0.6	190.± 11.	81.± 7.
00224	438.9	1.30± 0.06	3.36± 0.16	4.3± 0.3	7.7± 0.8	30.5± 0.7	27.9± 1.3	253.± 10.	193.± 15.
00342	19.3	0.64± 0.06	0.52± 0.04	1.6± 0.1	1.6± 0.2	12.0± 0.3	7.9± 0.4	185.± 8.	76.± 6.
00598	15.4	7.66± 2.94	0.22± 0.11	6.1± 2.1	0.5± 0.3	8.5± 0.2	2.4± 0.1	124.± 5.	23.± 2.
00660	23.3	0.57± 0.05	0.94± 0.07	0.6± 0.2	0.2± 0.1	9.2± 0.2	3.8± 0.2	147.± 6.	37.± 3.
00891	24.8	0.71± 0.05	1.84± 0.13	3.1± 0.4	3.1± 0.5	6.4± 0.2	3.1± 0.3	144.± 11.	35.± 4.
01365	31.1	0.90± 0.09	2.51± 0.18	3.3± 0.2	6.6± 0.8	14.4± 0.3	10.4± 0.9	199.± 16.	95.± 10.
01808	16.0	0.66± 0.06	1.38± 0.10	3.0± 0.3	3.2± 0.4	2.0± 0.0	0.4± 0.0	77.± 8.	6.± 1.
02403	19.7	0.14± 0.05	0.02± 0.00	0.2± 0.0	0.0± 0.0	7.6± 0.2	2.9± 0.1	135.± 6.	29.± 2.
02903	23.8	2.50± 0.30	5.24± 0.63	3.8± 0.5	8.0± 1.3	7.6± 0.5	5.0± 1.0	168.± 33.	56.± 16.
03079	21.3	0.69± 0.07	2.63± 0.19	3.8± 0.6	4.4± 0.8	16.2± 1.2	9.5± 1.6	189.± 30.	80.± 21.
03198	31.1	6.21± 1.46	0.50± 0.10	3.1± 0.2	1.6± 0.2	13.4± 0.3	6.2± 0.5	166.± 13.	54.± 6.
03628	14.2	0.84± 0.08	1.52± 0.11	3.6± 0.4	3.6± 0.5	8.5± 0.2	4.8± 0.4	162.± 13.	51.± 5.
04258	29.2	0.47± 0.04	1.19± 0.09	0.8± 0.1	0.9± 0.1	19.4± 0.5	16.1± 1.0	225.± 13.	134.± 12.
04321	25.6	1.32± 0.09	2.76± 0.20	7.6± 0.5	16.8± 1.6	7.1± 0.2	4.2± 0.3	159.± 13.	48.± 5.
04527	12.8	0.41± 0.08	0.94± 0.13	2.6± 0.8	1.7± 0.6	12.2± 1.5	7.4± 2.0	181.± 43.	70.± 29.
04565	34.1	3.05± 0.28	6.40± 0.76	4.0± 0.8	4.6± 1.2	19.2± 1.4	16.3± 2.8	226.± 35.	137.± 35.
04736	10.4	0.82± 0.12	1.09± 0.13	0.9± 0.2	0.8± 0.2	7.3± 0.7	2.3± 0.5	125.± 27.	23.± 8.
04945	20.0	0.36± 0.04	0.69± 0.07	0.3± 0.1	0.3± 0.0	9.0± 0.2	5.6± 0.3	170.± 10.	59.± 5.
05033	35.1	1.04± 0.10	3.76± 0.27	5.7± 0.7	11.4± 1.6	38.9± 2.8	41.2± 7.1	280.± 44.	262.± 68.
05055	39.4	2.96± 0.21	4.15± 0.30	1.8± 0.3	1.7± 0.2	7.7± 0.2	4.2± 0.3	156.± 9.	45.± 4.
05236	39.3	0.19± 0.04	0.47± 0.06	3.0± 0.7	1.8± 0.5	8.1± 0.2	4.4± 0.4	158.± 12.	47.± 5.
05457	13.5	2.76± 0.41	2.90± 0.41	2.4± 0.5	2.2± 0.5	8.1± 0.6	4.6± 0.9	161.± 28.	50.± 13.
05907	28.6	1.60± 0.08	2.76± 0.13	6.9± 0.5	13.8± 1.0	6.7± 0.2	3.4± 0.2	148.± 6.	39.± 3.
06946	17.0	0.36± 0.04	0.92± 0.07	3.8± 0.5	4.2± 0.6	9.4± 0.2	5.6± 0.5	169.± 13.	58.± 6.
03521	23.6	0.72± 0.09	1.52± 0.15	1.6± 0.2	3.5± 0.3	22.6± 1.6	14.0± 2.4	206.± 32.	103.± 26.
04303	25.3	0.33± 0.14	0.15± 0.05	2.1± 0.5	1.1± 0.3	11.9± 0.9	4.5± 0.8	148.± 26.	39.± 10.
04569	14.9	1.39± 0.37	0.66± 0.18	12.0± 0.9	39.7± 5.8	9.8± 1.6	3.5± 1.3	140.± 47.	33.± 19.
00253	14.2	0.93± 0.09	1.60± 0.11	1.9± 0.3	1.9± 0.4	7.9± 0.6	3.5± 0.6	145.± 23.	36.± 9.
00508	25.7	2.89± 1.31	2.12± 0.84	6.6± 0.5	25.1± 3.0	87.1± 10.4	239.3± 59.7	479.± 105.	1271.± 515.
04273	13.0	0.99± 0.94	0.15± 0.08	3.8± 0.3	4.0± 0.5	20.6± 1.5	14.1± 2.2	210.± 29.	110.± 27.
02916	36.9	1.56± 0.22	2.18± 0.26	2.8± 0.6	2.6± 0.5	11.4± 0.3	7.5± 0.6	183.± 14.	73.± 8.
03993	53.6	4.35± 0.31	16.59± 1.19	4.8± 0.7	7.5± 1.3	135.1± 3.2	214.9± 17.7	392.± 31.	687.± 83.

Table 2. Mean parameters for selected galaxies[†].

Number of galaxies	N	43
Bulge scale radius	$a_{\rm b}$ (kpc)	1.5± 0.2
— mass	$M_{\rm b}(10^{10}M_{\odot})$	2.3± 0.4
Disk scale radius	$a_{\rm d}$(kpc)	3.3± 0.3
— mass	$M_{\rm d}(10^{10}M_{\odot})$	5.7± 1.1
Dark Halo scale radius	h (kpc)	21.6± 3.9
— mass within h	$M_{\rm h}(10^{10}M_{\odot})$	22.3± 7.3
— critical radius	R_{200} (kpc)	193.7± 10.8
— critical mass	$M_{200}(10^{10}M_{\odot})$	127.6± 32.0
B+D mass.....	$M_{\rm b+d}(10^{10}M_{\odot})$	7.9± 1.2
B+D+H mass.....	$M_{200+{\rm b}+{\rm d}}(10^{10}M_{\odot})$	135.6± 32.0
(B+D)/Halo mass ratio	$M_{\rm b+d}/M_{200}$	0.062±0.018
(B+D)/Total mass ratio	$M_{\rm b+d}/M_{200+{\rm b}+{\rm d}}$	0.059± 0.016

Table 3. Spearman's rank correlation coefficient $\rho_{\rm S}$, linear correlation coefficient r for log-log plots, and probability $P(r;N)$ for the coefficient exceeding r from uncorrelated sample. The number of sample galaxies is $N = 43$.

param 1	param 2	$\rho_{\rm S}$	r	$P(r;N)$
$a_{\rm b}$	$a_{\rm d}$	0.56	0.54	0.0002
$a_{\rm b}$	h	0.16	0.28	0.07
$a_{\rm b}$	R_{200}	0.19	0.26	0.09
$a_{\rm d}$	h	0.08	0.16	0.31
$a_{\rm d}$	R_{200}	0.11	0.16	0.31
h	R_{200}	0.90	0.94	0
$M_{\rm b}$	$M_{\rm d}$	0.63	0.62	6×10^{-5}
$M_{\rm b}$	$M_{\rm h}$	0.29	0.34	0.03
$M_{\rm b}$	M_{200}	0.34	0.34	0.03
$M_{\rm d}$	$M_{\rm h}$	0.32	0.35	0.02
$M_{\rm d}$	M_{200}	0.33	0.34	0.03
$M_{\rm h}$	M_{200}	0.99	0.98	0
$a_{\rm b}$	$M_{\rm b}$	0.55	0.47	0.001
$a_{\rm d}$	$M_{\rm d}$	0.84	0.87	0
h	$M_{\rm h}$	0.94	0.98	0
R_{200}	M_{200}	1.00	1.00	0

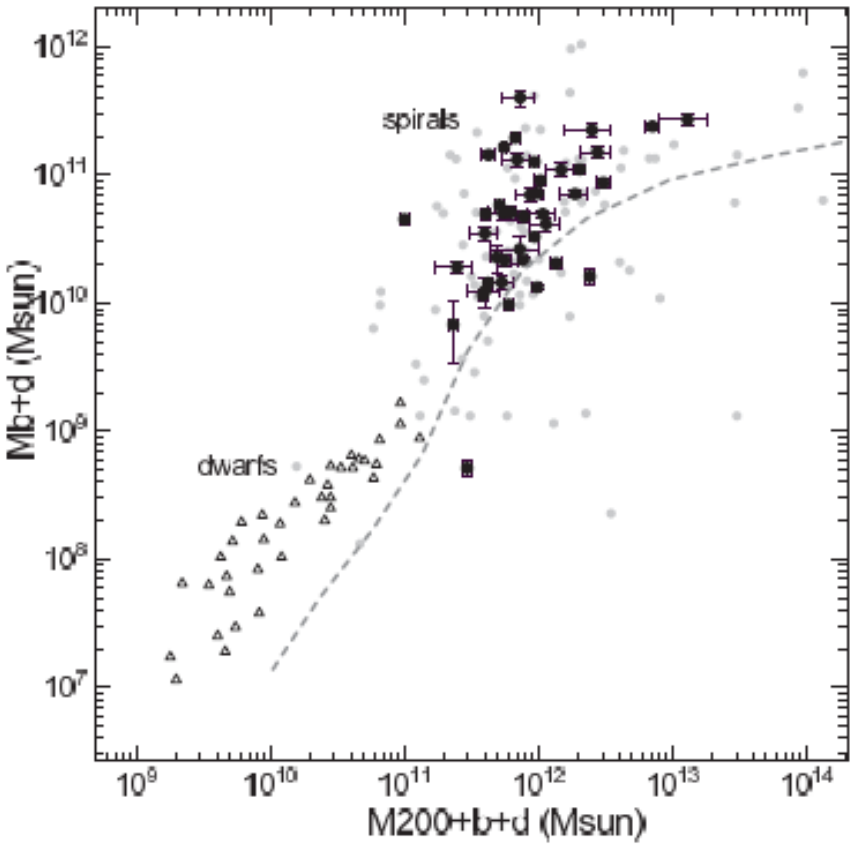

Fig. 7. $M_{\rm b+d}$-$M_{\rm 200+b+d}$ relation compared with the stellar vs. total mass relation for dwarf galaxies (triangle: Miller et al. 2014) and simulation (gray dashed line: Behroozi et al. 2013). Black dots are the selected galaxies with reasonable fitting results, while small gray dots (including black dots) show non-weighted results from automatic decomposition of all rotation curves.

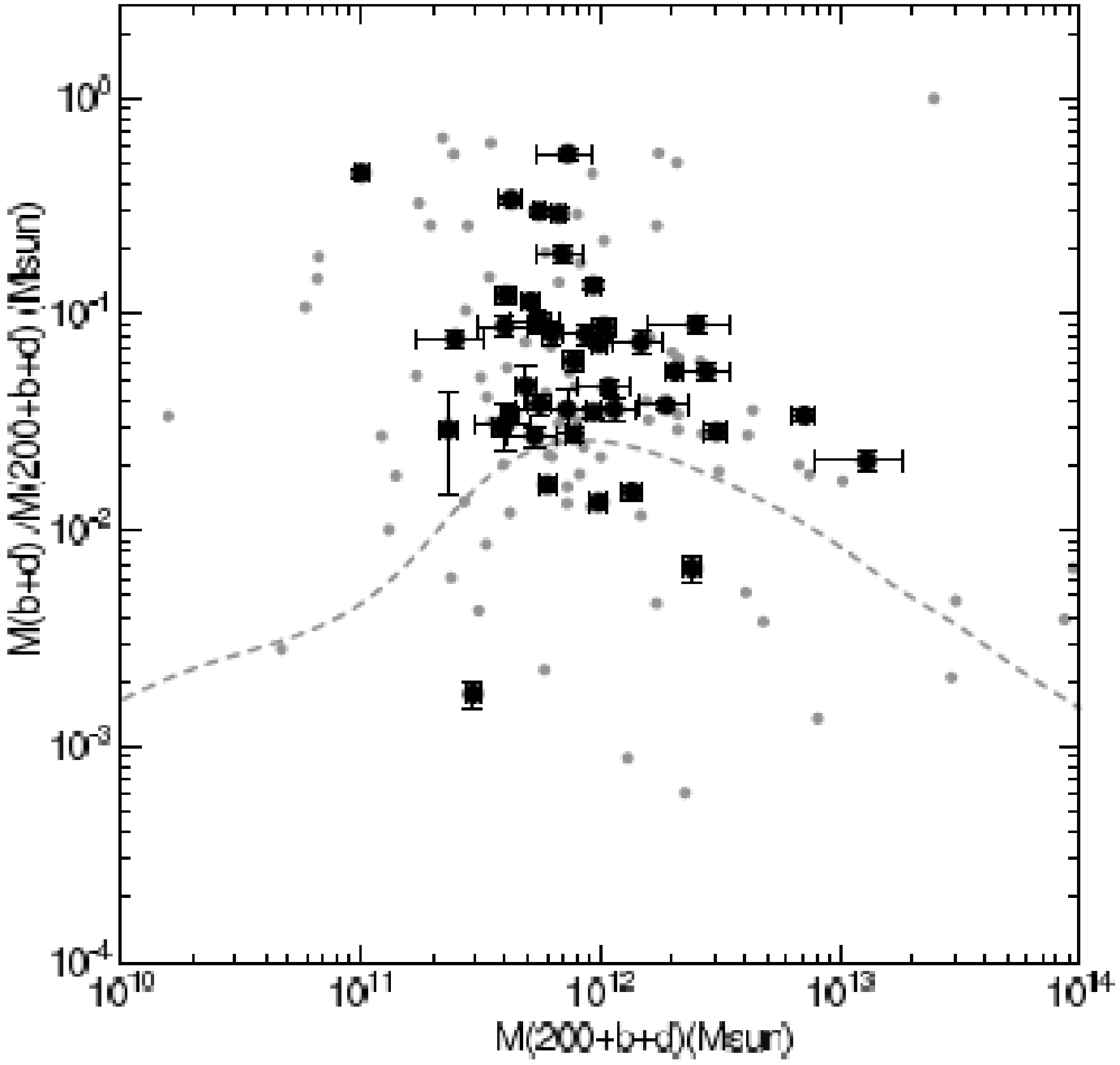
M(b+d) /M(200+b+d) (Msun)
M(200+b+d)(Msun)
10^{0}
10^{-1}
10^{-2}
10^{-3}
10^{-4}
10^{10}
10^{11}
10^{12}
10^{13}
10^{14}

The bulge+disk mass to dark halo mass ratio of spiral galaxies is compared with that for dwarf alaxies, and the observed ratios are higher than that from simulations by a factor of three.

QUASARS PROBING QUASARS VIII. THE PHYSICAL PROPERTIES OF THE COOL CIRCUMGALACTIC MEDIUM SURROUNDING $Z \sim 2$–3 MASSIVE GALAXIES

Marie Wingyee Lau[1,2], J. Xavier Prochaska[2], Joseph F. Hennawi[3]

Draft version October 24, 2015

ABSTRACT

We characterize the physical properties of the cool $T \sim 10^4$ K circumgalactic medium surrounding $z \sim$2–3 quasar host galaxies, which are predicted to evolve into present day massive ellipticals. Using a statistical sample of 14 quasar pairs with projected separation < 300 kpc and high dispersion, high S/N spectra, we find extreme kinematics with low metal ion lines typically spanning ≈ 500 km s^{-1}, exceeding any previously studied galactic population. The CGM is significantly enriched, even beyond the virial radius, with a median metallicity [M/H] ≈ -0.6. The α/Fe abundance ratio is enhanced, suggesting that halo gas is primarily enriched by Type II supernovae. The total mass of the cool CGM is estimated to be 1.9×10^{11} M$_\odot$ $(R_\perp/160$ kpc$)^2$, accounting for $\approx 1/3$ of the galaxy halo baryonic budget. The ionization state of CGM gas increases with projected distance from the foreground quasars, contrary to expectation if the quasar dominates the ionizing radiation flux. However, we also found peculiarities not exhibited in the CGM of other galaxy populations. In one absorption system, we may be detecting unresolved fluorescent Lyα emission, and another system shows strong N V lines. Taken together these anomalies suggest that transverse sightlines are at least in some cases possibly illuminated. We also discovered a peculiar case where detection of the C II fine structure line implies an electron density > 100 cm^{-3} and subparsec scale gas clumps.

Subject headings: galaxies: formation – quasars: general – quasars: absorption lines – intergalactic medium – circumgalactic medium – Lyman limit systems – SDSS

1. INTRODUCTION

The circumgalactic medium (CGM) is defined as the gaseous halo extending approximately 20–300 kpc from galaxies. It is the site of interplay between outflows from galaxies and accretion onto galaxies, and the impact of these processes on galaxy evolution and the enrichment of the intergalactic medium (IGM) remain open questions. Galactic scale outflows are ubiquitous (Weiner

phase CGM traced by O VI is also observed for individual galaxy halos (Tumlinson et al. 2011; Peeples et al. 2014), but is generally too faint to observe in isolated galaxies (e.g. Mulchaey et al. 1996; Anderson & Bregman 2011). For our Milky Way, the presence of a warm-hot phase halo can be inferred from matching O VII absorption in extragalactic sightlines and soft X-ray emission background (Bregman & Lloyd-Davies 2007; Wang et al. 2005). It can also be inferred from observations

From a total of 700 confirmed pairs, we selected 14pairs with projected separations < 300 kpc and high dispersion, high S/N data, to study the CGM surrounding quasars at z ~2-3. We analyzed the velocity fields of the absorbing gas, the H I and metal ion column densities and the ionization state characterized by the ionization parameter U.

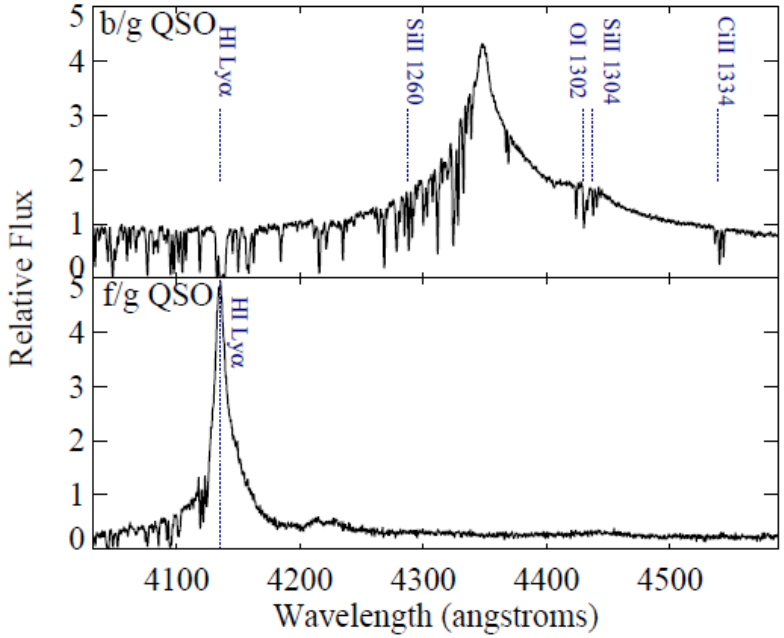

FIG. 1.— We show J0853-0011 as an example of a background-

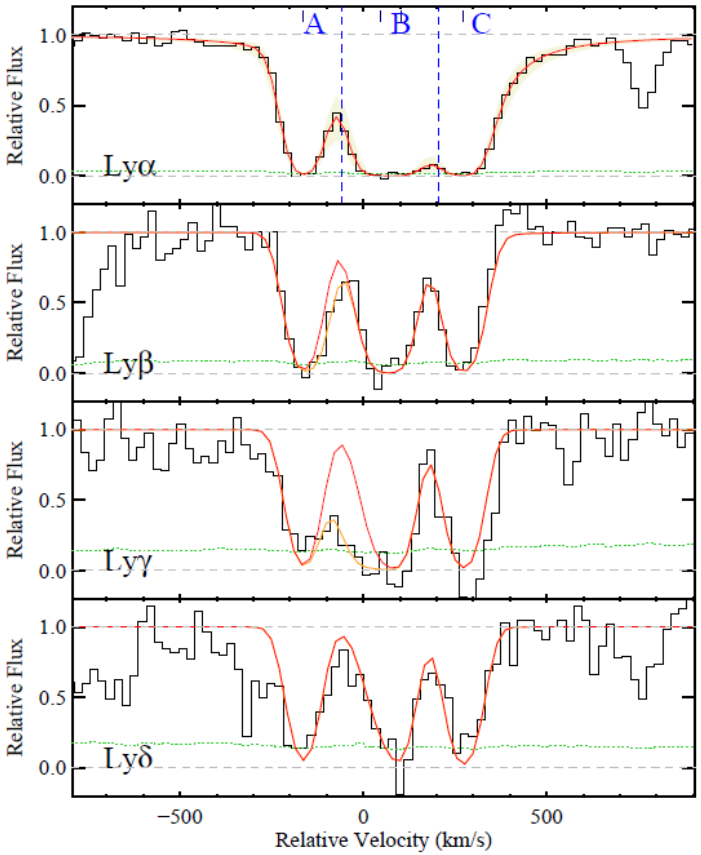

FIG. 4.— Example fit to H I Lyman series absorption profiles for J0853-0011. The black histograms show the Lyman series identified in the J0853-0011BG spectrum at velocities consistent with

- The ionization parameter U positively correlates with projected distance from the foreground quasar. This runs contrary to expectation should the foreground quasar dominate the ionizing radiation field.

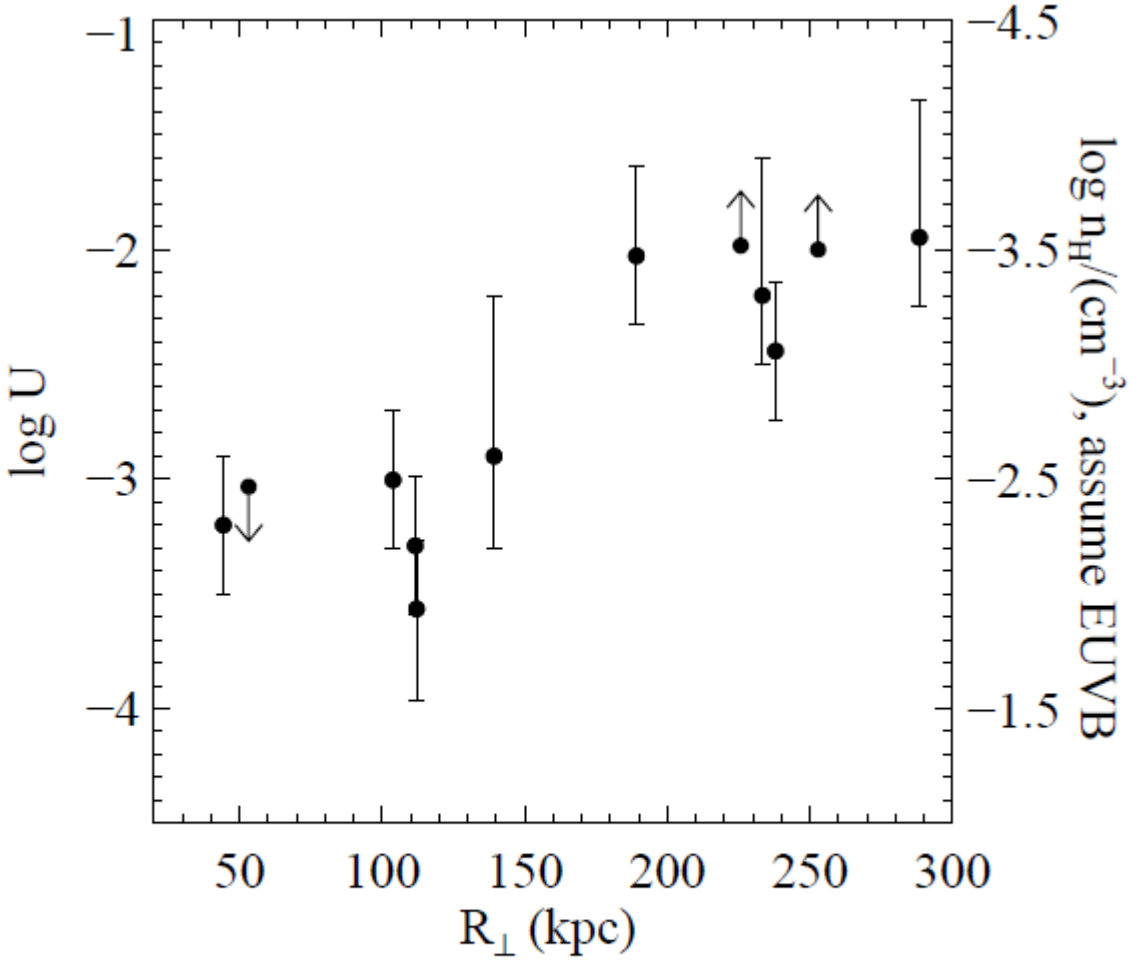

FIG. 7.— $< U >$ as a function of $R_\perp$. We estimated a characteristic average $< U >$ for each quasar associated absorption system

- The CGM is significantly enriched even beyond the estimated virial radius of the host dark matter halos (160 kpc). Within R~ 200 kpc, the median metallicity is [M/H] = □ 0:6 dex. The O/Fe ratio is supersolar in nearly all cases.

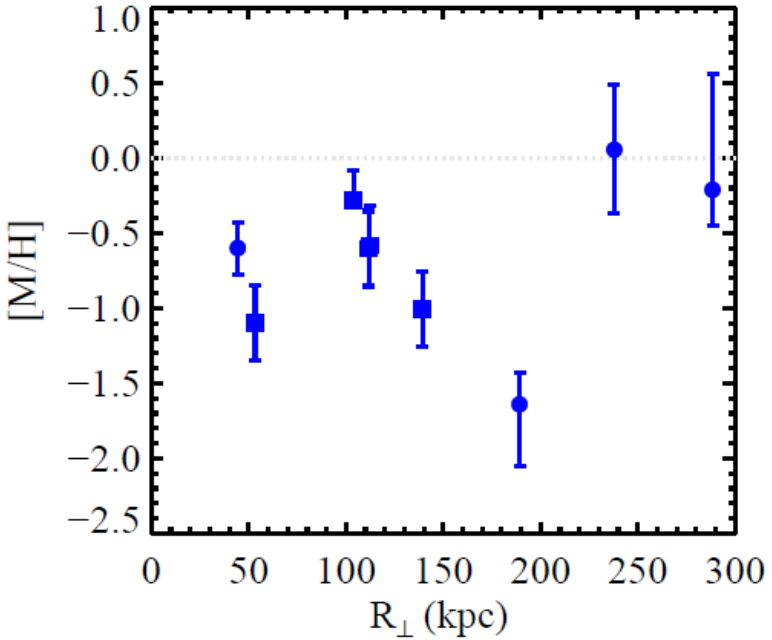

FIG. 11.— All metallicity estimates for the cool gas of the full sample, estimated from the O I, Si II, Si III or Si IV columns with ionization corrections from Cloudy. All measurements exceed 1/10 solar and the median [M/H]= −0.59 dex. The measurements exhibits no correlation with N_{HI} or $R_\perp$. Significant enrichment exists even beyond the estimated virial radius of the host halos at ≈ 160 kpc. Note in the [M/H] versus $R_\perp$ subplot, there are two almost overlapping points at $R_\perp = 112$ kpc.

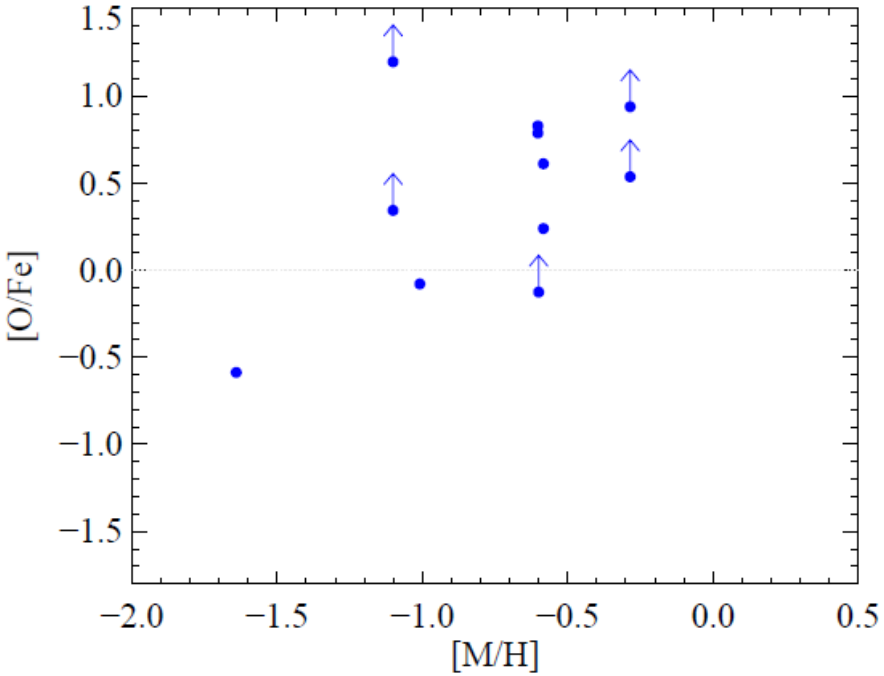

FIG. 12.— [O/Fe] estimates after adopting the ionization corrections to O^0/Fe^+. Nearly all measurements indicate supersolar O/Fe ratio, implying a significant fraction of the CGM surrounding quasars must have enhanced α/Fe abundance. Our findings suggest a star formation history similar to elliptical galaxies and a starburst that lasted less than 1 Gyr.

- Within the estimated virial radius, we found the total mass of the cool phase CGM is substantial: M^{CGM}_{cool} ~1.5*10^{11} Mc (R<160 kpc)^2. This accounts for 1/3 of the dark halo baryonic budget.

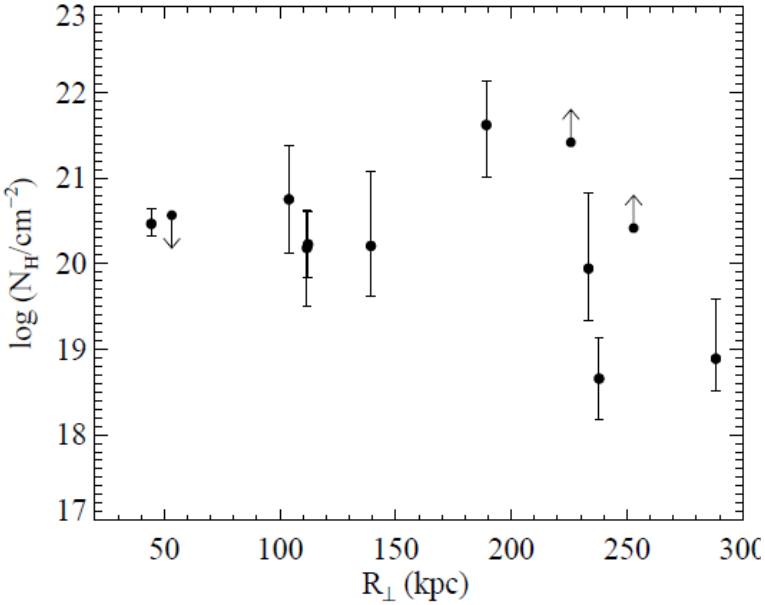

FIG. 15.— The total H column from ionization state modeling as a function of $R_\perp$. We see little evolution in N_H up to ≈ 200 kpc, as both N_{HI} and the neutral fraction x_{HI} anticorrelate with $R_\perp$. The median $N_H = 10^{20.5}$ cm^{-2}.

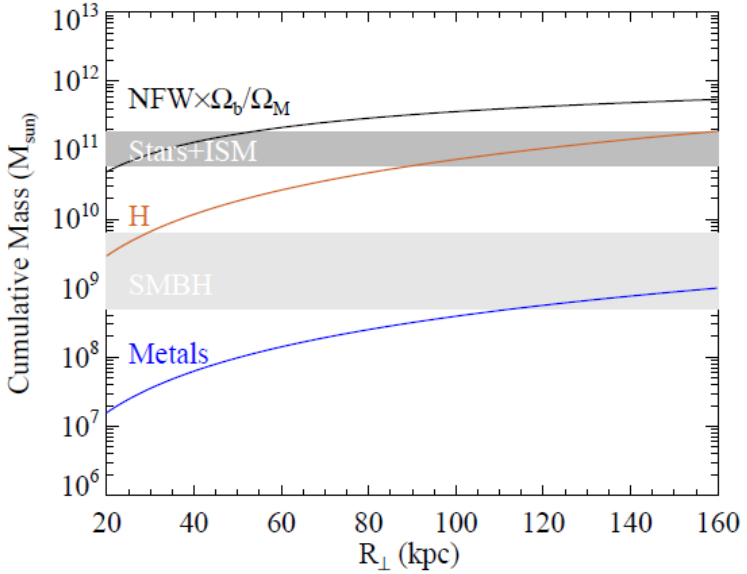

FIG. 16.— Using the median N_H and the median [M/H] within 200 kpc, we constructed cumulative mass profiles of total H and metals in the cool CGM. For reference we also included the expected baryonic mass projected profile of an NFW halo with $c = 4$ and dark matter mass $M_{DM} = 10^{12.5}$ M$_\odot$ $(R_\perp/160$ kpc$)^2$. We also plotted the typical host galaxy mass, as well as the range of supermassive black hole mass of the QPQ8 sample. We estimated the total mass of the cool CGM as $M^{CGM}_{cool} \approx 1.9 \times 10^{11}$ M$_\odot$ $(R_\perp/160$ kpc$)^2$. This accounts for 1/3 of the total expected baryonic mass.